ARTICLES

Purification of Boron Nitride Nanotubes through Polymer Wrapping

Chunyi Zhi,*,† Yoshio Bando,† Chengchun Tang,† Susumu Honda,‡ Kazuhiko Sato,‡ Hiroaki Kuwahara,‡ and Dmitri Golberg†

Advanced Materials Laboratory, National Institute for Materials Science (NIMS), Namiki 1-1, Tsukuba, Ibaraki 305-0044, Japan, and Innovation Research Institute, Teijin Ltd., 2-1, Hinode-cho, Iwakuni, Yamaguchi

Received: September 1, 2005; In Final Form: October 25, 2005

An effective method was proposed to remove obstinate boron nitride phase impurities in boron nitride nanotubes (BNNTs). The method is based on strong interactions between BNNTs and a conjugated polymer wrapping them and significant weight and size difference between BNNTs and impurities. The as-grown samples and purified samples were compared through detailed characterization, using scanning electron microscopy, transmission electron microscopy, and Raman and Fourier transformed infrared spectroscopy. The results reveal that impurities are effectively removed and resultant BNNTs possess perfect crystallization.

I. Introduction

Boron nitride nanotubes (BNNTs) were synthesized by Chopra et al. for the first time in 1995.[1] Opposed to a carbon nanotube (CNT), whose electrical performance is a complex function of NT structural parameters, BNNT is a stable wide-band gap semiconductor independent of diameter and chirality.[2] In addition, BNNT possesses a high chemical stability. It is inert to most acids and alkalis and has a superb resistance to oxidation.[3] Moreover, BNNTs display excellent mechanical properties and high thermal conductivity.[4−6] All these factors make BNNTs highly useful in nanotube-based materials and devices working in oxidative and hazardous environments and/or at high temperatures. However, although CNTs are easy to fabricate now, the study progress of BNNTs is hampered because of the difficulties in obtaining highly pure BNNTs in large quantity.

Many methods have been developed for the synthesis of BNNTs, such as arc-discharge,[1,7] laser ablation,[8] ball-milling,[9] and substitution chemical reactions.[10] Some of these methods yield large quantities of BNNTs, but the purity is still a concern.[9] By using a chemical vapor deposition with a boron oxide as a reactant (BOCVD),[11,12] the yield of highly pure BNNTs can reach hundreds of milligrams in a single experimental run. A higher temperature (∼1500−1700 °C) was found useful for the yield increase. However if the synthesis temperature becomes too high (1900 °C or more), insurmountable impurities contaminate a sample, even if the optimal precursor is in use.

For CNTs, many purification methods have been developed, such as strong acid oxidation,[13] gas-phase oxidation,[14,15] microwave heating,[16,17] organic functionalization,[18] etc. Various methods have been used to characterize the sample before and after the purification process, such as Raman and thermal gravimetric analysis (TGA), etc. The oxidation process can remove catalyst particles and some amorphous carbon effectively. However, it is extremely difficult to purify BNNTs: although catalyst particles may be removed by acid wash, other BN phase impurities are hard to be removed because BN is structurally stable and oxidation resistant. To the best of our knowledge, no purification-related work has been performed for BNNTs until now.

Recently, soluble BNNTs are fabricated by wrapping them with a conjugated polymer, poly(*m*-phenylenevinylene-*co*-2,5-dioctoxy-*p*-phenylenevinylene) (PmPV).[19] The structure of PmPV is similar to that of a standard polyphenylenevinylene. A chain of this type of the polymer tends to coil, thus forming a helical structure. It is thought that the coiled polymer conformation easily makes the nanotubes wrap with the polymer. This, in turn, leads to the intermolecular proximity and occurrence of the prominent $\pi-\pi$ interactions. A similar phenomenon has been observed during functionalization of CNTs.[20] BNNTs may have stronger interactions with PmPV as compared with CNTs. This has indeed been proved during cathodoluminescence experiments.[19] On the basis of this, in the present paper we propose a novel alternative method for BNNT purification. Before its detailed description a research effort has to be made to clarify which impurities are peculiar to a standard BNNT sample. Figure 1a is a typical scanning electron microscopy (SEM) image of BNNT synthesized at 1900 °C with BOCVD method. It can be seen that in addition to BNNTs with diameters of approximately 50 nm, there are many particles and fibers of larger diameters (hundreds of nanometers or more). Detailed electron energy loss spectra investigations reveal that these impurities are also made of boron nitride. In addition, some metal catalyst particles (Mg, Fe, etc.) can also be found in the as-grown sample. They can be removed through washing with acid. In BNNTs synthesized by other methods, for instance, a substitution reaction,[21] carbon may be introduced, which also can be removed via heating a sample in air.

* Address correspondence to this author. E-mail: zhi.chunyi@nims.go.jp.
† National Institute for Materials Science.
‡ Innovation Research Institute.

10.1021/jp054941f CCC: $33.50
Published on Web 01/11/2006

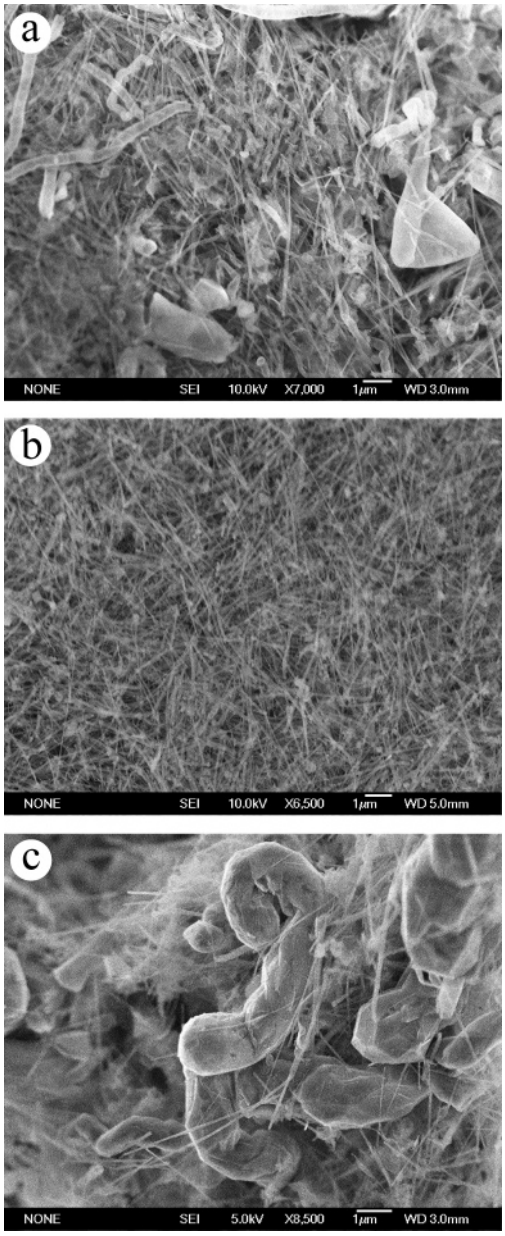

Figure 1. SEM images of (a) as-grown, (b) purified, and (c) insoluble material BN samples.

For the BNNT samples discussed in the present paper the sole impurities were found to be boron nitride particle and fibers with large diameters. Herein we propose an effective method to remove these impurities. The as-grown samples and purified samples were compared through detailed characterization by using scanning electron microscopy (SEM), transmission electron microscopy (TEM), and Raman and Fourier transformed infrared (FTIR) spectroscopy to confirm the desired purification.

II. Experimental Section

BNNTs were synthesized by the BOCVD method; the detailed growth procedure was reported elsewhere.[11,12] Briefly, a mixture of MgO, FeO, and boron powder was heated in a boron nitride crucible to 1900 °C. The heating yields Mg, Fe vapors, and B_2O_2, which are transported by an Ar gas and meet with ammonia. After synthesis for over 2 h, a white product was collected from the boron nitride crucible. The high synthesis temperature, up to 1900 °C, was selected in the present experiment in order to increase the nanotube yield; however, impurities significantly contaminate the samples in this case. The purification process is schematically shown in Figure 2. First, the as-grown BNNTs were washed by HNO_3 to first remove the catalytic particles, such as Fe, Mg, etc. A typical SEM image of a washed sample is shown in Figure 1a, which indicates that a significant fraction of BN particles and fibers is still present. To further purify the samples, a conjugated polymer, PmPV, was used to wrap up the BNNTs. PmPV and BNNTs were mixed in chloroform and then the BNNTs were made soluble through subsequent sonication.[19] Then the mixture was centrifugalized (2000 rpm), accompanied by the removal of insoluble materials. The solvent was then evaporated and the PmPV−BNNT composite was fabricated. The last step was to heat treat the composite in air at 700 °C to remove PmPV wrappings and retract BNNTs (BNNTs can withstand up to 900−1000 °C in air according to the TGA).[19]

A SEM (JEOL SM67F) was used to check the product morphology. The microstructure was investigated with a JEOL-3000F high-resolution field-emission TEM operated at 300 kV. Raman spectra were collected in a backscattering geometry at room temperature with use of a Reinshaw 2000 Raman system. FTIR spectra were collected on a Perkin-Elmer FTIR spectrometer with a laser wavelength of 1024 nm.

III. Results and Discussion

Panels b and c of Figure 1 show typical SEM images of purified BNNTs and insoluble materials, respectively. Most BNNTs have a diameter of ~50 nm and length up to 10 μm, as shown in Figure 1b. A purified sample is obviously depleted in BN particles and fibers as compared to the as-grown sample. By contrast, an insoluble material sample is significantly enriched with the impurities. However, there are still many BNNTs remaining in the insoluble material sample. It is noted that these nanotubes can be further separated from the contaminants by repeating the purification process. During TEM, the effect of purification was particularly obvious. Panels a, b, and c of Figure 3 show TEM images of an original sample, a purified sample, and a sample containing insoluble materials. It can be seen that the impurities include particles, fibers, flakes, etc., which are present as the insoluble materials.

The principle of BNNT separation from the present impurities is based on the corresponding difference in weight and size and strong interactions between PmPV and BNNTs.[19] Due to the

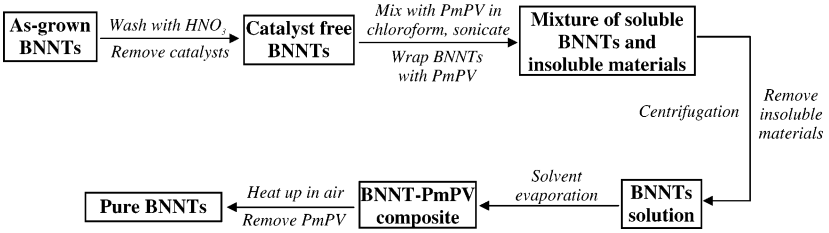

Figure 2. Schematic diagram for the process of purification.

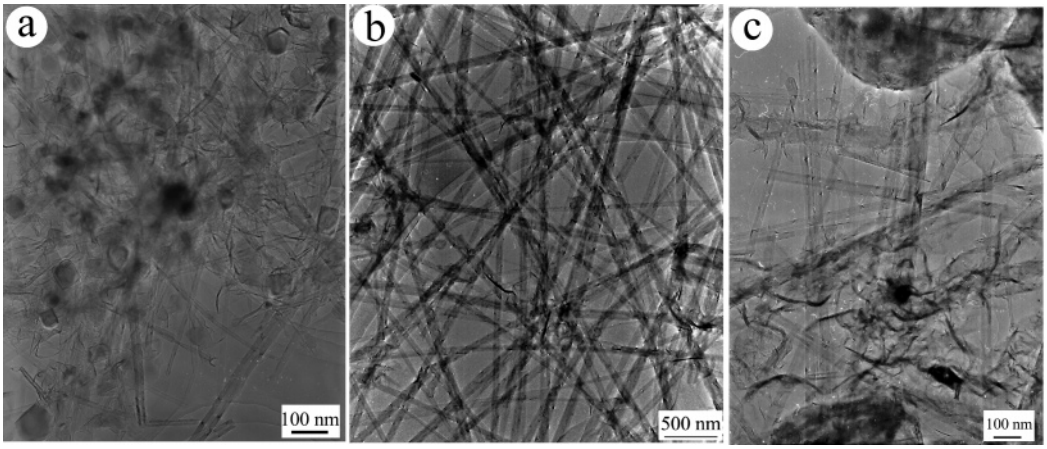

Figure 3. TEM images of (a) as-grown, (b) purified, and (c) insoluble material BN samples.

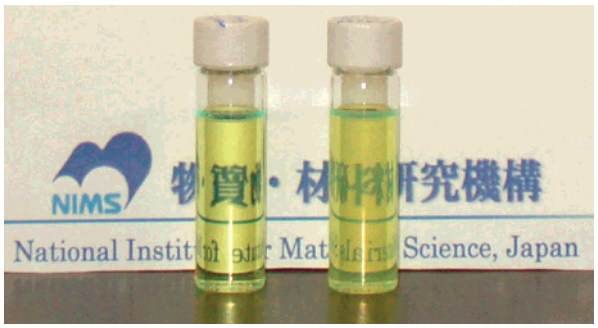

Figure 4. Image of PmPV/chloroform solution (left) and PmPV/BNNT/chloroform unsaturated homogeneous solution (right). The yellow color originates from PmPV.

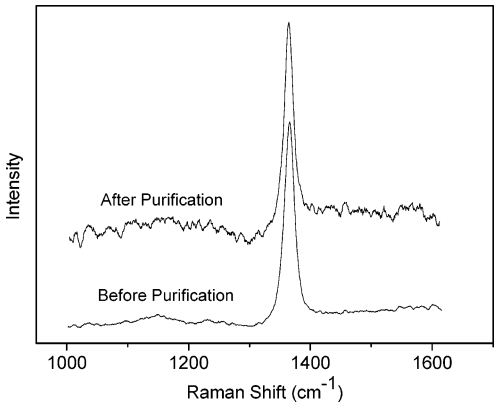

Figure 5. Raman spectra of BNNTs before and after purification.

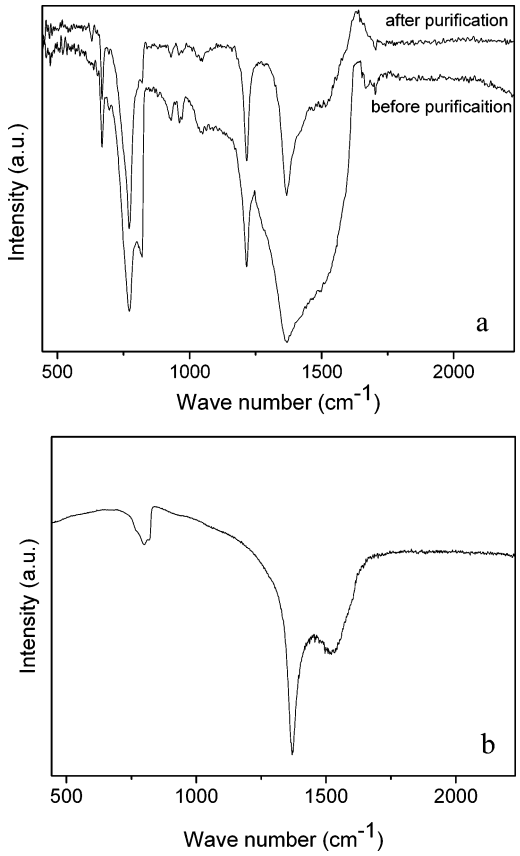

Figure 6. FTIR spectra of (a) BNNTs before and after purification; (b) highly pure BNNTs obtained by a low-temperature growth.

interaction, The BNNTs wrapped by PmPV can be suspended in chloroform, as shown in Figure 4.[19] No nanotube precipitation was observed during a long time suspension keeping at ambient conditions, whereas the impurities deposited at the vessel bottom due to a heavier weight. It should be noted that, using this method, BN flakes which have similar size and weight with BNNTs cannot be removed effectively, as revealed in Figure 3b.

Raman was used to investigate the crystallization of BNNTs before and after purification. In the case of CNTs, the intensity ratio of the G band to the D band was usually utilized to characterize crystallization and purity. Different from CNTs, only one dominate peak at around 1363 cm^{-1} was observed for BNNTs, which is attributed to the so-called E_{2g} mode, the well-known counterphase BN vibrational mode within the BN sheet. The FWHM of the peak slightly decreased (from 20 to 17 cm^{-1}), which indicates higher crystallization and purity are obtained in the purified sample.

Solution-phase FTIR was used to provide a quantitative comparison of BNNTs before and after purification since both TEM and SEM methods give sole selective area evaluation and an overall sample characterization cannot be readily made. Figure 6a shows FTIR spectra of BNNTs before and after purification. The peaks at 820, 1369, and 1514 cm^{-1} originate from BNNTs, which correspond to A_{2u} (B−N vibration perpendicular to the tube axis), E_{1u} (TO), and E_{1u} (LO) (B−N vibration parallel to the tube axis) modes, respectively.[22] Other peaks are coming from chloroform and PmPV. The variation

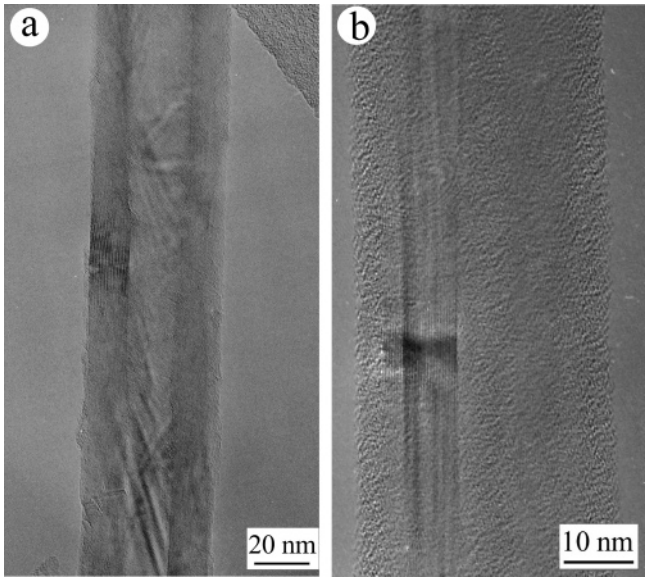

Figure 7. TEM images of (a) BNNTs retracted from the BNNT-PmPV composite and (b) BNNTs wrapped by PmPV.

of intensities and FWHM of the peaks indicates the notable difference of the sample quality. Splitting between longitudinal and transverse optical modes (LO-TO splitting) in FTIR spectra of BNNTs is induced by a macroscopic electric field E for longitudinal optical phonons in the limit $q \rightarrow 0$. The relative spectral weight of LO and TO peaks is related to the mixture of the oscillator strength of the modes parallel and perpendicular to the *c*-axes of *h*-BN. In a polycrystalline *h*-BN sample, a three-dimensional disorder results in a very weak LO-TO splitting, with only a dominate peak at 1377 cm^{-1} being observed.[23] In the FTIR spectra of purified BNNTs, the E_{1u} peaks are only slightly split, and the FWHM of the dominate peak is $\sim$60 cm^{-1}, while in the spectra of unpurified BNNTs, prominent splitting is observed, and FWHM of the dominant peak drastically increases to $\sim$300 cm^{-1}. This comparison implies a much higher quality of the purified sample. To further confirm this statement, a solid-phase FTIR spectrum of highly pure BNNTs fabricated through BOCVD at a lower temperature of 1300 °C is depicted in Figure 6b. The features of E_{1u} peaks are similar to those in purified BNNTs, while quite distinct from those of BNNTs before purification. This result clearly confirms the effect of purification. We also note that the intensity of the A_{2u} peak at 820 cm^{-1} significantly decreases after purification making the spectrum similar to that of BNNTs grown at the low temperature and to that of the polycrystalline *h*-BN sample. It is obvious that this feature is an additional proof of the purification effect, while the detailed mechanism is still not clear.

The BNNTs were retracted from the solutions during heating to 60 °C (to evaporate away chloroform) and then at 700 °C over 30 min to fully remove PmPV. The color of the sample quickly turned from yellow (color of PmPV) to white (color of BNNTs), which indicated that PmPV had indeed been oxidized away. TEM was utilized to check a final sample. The surfaces of the recovered BNNTs became clean, as shown in Figure 7a. By contrast, before annealing, BNNTs wrapped by PmPV due to strong $\pi-\pi$ interactions display the images shown in Figure 7b. Importantly, the structure and morphology of retracted BNNTs was perfectly preserved since the used wrapping treatment is a noncovalent functionalization.

IV. Conclusion

In summary, a novel purification method of boron nitride nanotubes was developed. During purification the effective removal of BN particles and fibers with large diameters took place. The separation of BNNTs from impurities is based on a significant difference in weight and size and strong interactions between BNNTs and PmPV wrapping them. The samples before and after purification were compared by using SEM, TEM Raman, and FTIR techniques, which all indicate that impurities are effectively removed and resultant BNNTs possess perfect crystallization. The designed purification method is thought to be most important for the mass-production of BNNTs, fabrication of BNNTs composites, and integration of BNNTs into modern nanotechnology.

Acknowledgment. The authors thank Dr. Y. Uemura, Dr. M. Mitome, K. Kurashima, and R. Z. Ma for their cooperation and kind help.

Note Added after ASAP Publication. This manuscript was originally published on the Web January 11, 2006 with the captions to Figures 3 and 4 transposed. The corrected version of this manuscript was reposted January 18, 2006.

References and Notes

(1) Chopra, N. G.; Luyken, R. J.; Cherrey, K.; Crespi, V. H.; Cohen, M. L.; Louie, S. G.; Zettl, A. *Science* **1995**, *269*, 966.

(2) Rubio, A.; Corkill, J. L.; Cohen, M. L. *Phys. Rev. B* **1994**, *49*, 5081.

(3) Golberg, D.; Bando, Y.; Kurashima, K.; Sato, T. *Scr. Mater.* **2001**, *44*, 1561.

(4) Hernandez, E.; Goze, C.; Bernier, P.; Rubio, A. *Phys. Rev. Lett.* **1998**, *80*, 4502.

(5) Xiao, Y.; Yan, X. H.; Cao, J. X.; Ding, J. W.; Mao, Y. L.; Xiang, J. *Phys. Rev. B* **2004**, *69*, 205415.

(6) Chang, C. W.; Han, W. Q.; Zettl, A. *Appl. Phys. Lett.* **2005**, *86*, 173102.

(7) Loiseau, A.; Willaime, F.; Demoncy, N.; Hug, G.; Pascard, H. *Phys. Rev. Lett.* **1996**, *76*, 4737.

(8) Laude, T.; Matsui, Y.; Marraud, A.; Jouffrey, B. *Appl. Phys. Lett.* **2000**, *76*, 3239.

(9) Chen, Y.; Chadderton, L. T.; Gerald, J. F.; Williams, J. S. *Appl. Phys. Lett.* **1999**, *74*, 2960.

(10) Golberg, D.; Bando, Y. *Appl. Phys. Lett.* **2001**, *79*, 415.

(11) Tang, C.; Bando, Y.; Sato, T.; Kurashima, K. *Chem. Commun.* **2002**, 1290.

(12) Zhi, C. Y.; Bando, Y.; Tang, C.; Golberg, D. *Solid State Commun.* **2005**, *135*, 67.

(13) Ko, F.; Lee, C.; Ko, C.; Chu, T. *Carbon* **2005**, *43*, 727.

(14) Sen, R.; Rickard, S. M.; Itkis, M. E.; Haddon, R. C. *Chem. Mater.* **2003**, *15*, 4273.

(15) Jeong, T.; Kim, W.; Hahn, Y. *Chem. Phys. Lett.* **2001**, *344*, 18.

(16) Harutyunyan, A. R.; Pradhan, B. K.; Chang, J.; Chen, G.; Eklund, P. C. *J. Phys. Chem. B* **2002**, *106*, 8671.

(17) Vázquez, E.; Georgakilas, V.; Prato, M. *Chem. Commun.* **2002**, 2308.

(18) Georgakilas, V.; Voulgaris, D.; Vázquez, E.; Prato, M.; Guldi, D. M.; Kukovecz, A.; Kuzmany, H. *J. Am. Chem. Soc.* **2002**, *124*, 14318.

(19) Zhi, C. Y.; Bando, Y.; Tang, C.; Golberg, D.; Xie, R.; Sekiguchi, T. *J. Am. Chem. Soc.* Accepted for publication.

(20) (a) Star, A.; Stoddart, J. F.; Steuerman, D.; Diehl, M.; Boukai, A.; Wong, E. W.; Yang, X.; Chung, S. W.; Choi, H.; Heath, J. R. *Angew. Chem., Int. Ed.* **2001**, 40, 1721. (b) Curran, S. A.; Ajayan, P. M.; Blau, W. J.; Carroll, D. L.; Coleman, J. N.; Dalton, A. B.; Davey, A. P.; Drury, A.; McCarthy, B.; Maier, S.; Strevens, A. *Adv. Mater.* **1998**, *10*, 1091. (c) Coleman, J. N.; Dalton, A. B.; Curran, S.; Rubio, A.; Davey, A. P.; Drury, A.; McCarthy, B.; Lahr, B.; Ajayan, P. M.; Roth, S.; Barklie, R. C.; Blau, W. J. *Adv. Mater.* **2000**, *12*, 213.

(21) Han, W. Q.; Mickelson, W.; Cumings, J.; Zettl, A. *Appl. Phys. Lett.* **2002**, *81*, 1110.

(22) Zhi, C. Y.; Bando, Y.; Tang, C.; Golberg, D.; Xie, R.; Sekiguchi, T. *Appl. Phys. Lett.* **2005**, *86*, 213110.

(23) Borowiak-Palen, E.; Pichler, T.; Fuentes, G. G.; Bendjemill, B.; Liu, X.; Graff, A.; Behr, G.; Kalenczuk, R. J.; Knupfer, M.; Fink, J. *Chem. Commun.* **2003**, 82.